Science Advances
AAAS

Supplementary Materials for

A neurogenetic mechanism of experience-dependent suppression of aggression

Kenichi Ishii *et al.*

Corresponding author: Kenta Asahina, kasahina@salk.edu

Sci. Adv. **8**, eabg3203 (2022)
DOI: 10.1126/sciadv.abg3203

The PDF file includes:

Other Supplementary Material for this manuscript includes the following:

Supplementary Figure S1.

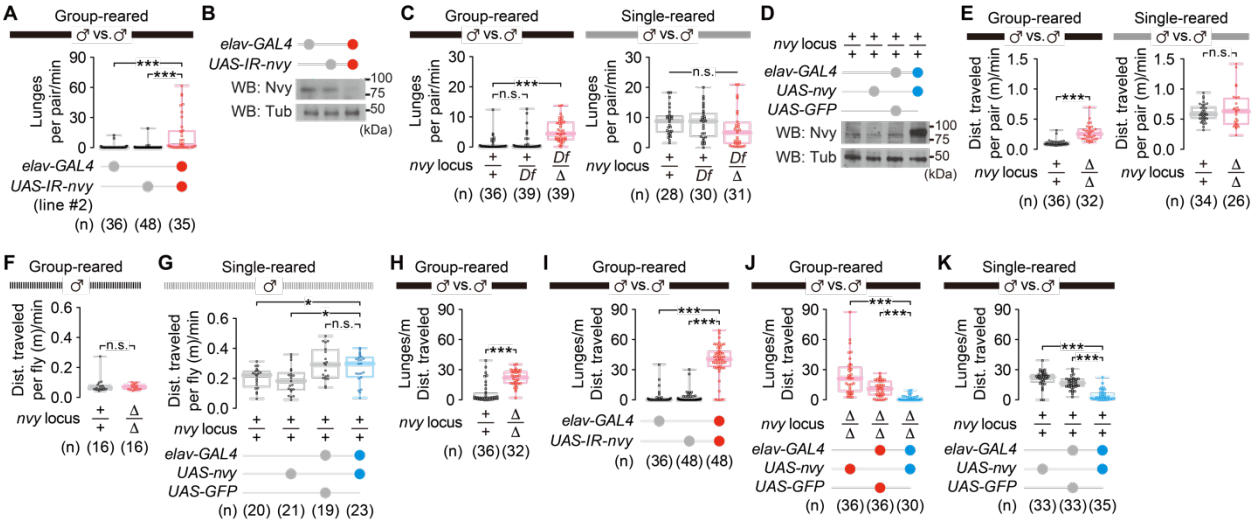

Fig. S1. Additional behavioral characterization of *nvy* mutants.

(**A**) Increased lunges performed by males following pan-neuronal *nvy* knockdown by another *UAS-IR* strain (JF03349). (**B**) Reduced expression of Nvy protein in fly heads following the pan-neuronal *nvy* knockdown, verified by Western blot. α-Tubulin (Tub) was used as an internal control. (**C**) Transheterozygous *nvy* mutation increased lunges in group-reared (left) but not in single-reared (right) males. Df, *Df(2R)Exel6082* (a deficiency that covers the *nvy* locus, see Fig. 1C); Δ, Δ*nvy*. (**D**) Pan-neuronal Nvy overexpression in fly heads verified by Western blot. (**E**) Distance traveled in pairs of Δ*nvy* males showed an increase after group-rearing (left) but not in single-rearing (right), similarly to lunge numbers. (**F**) Locomotion of solitary Δ*nvy* males (i.e., not as a pair) was comparable to the wild-type control. (**G**) Pan-neuronal *nvy* overexpression failed to impair the locomotion of solitary males. (**H to K**) Lunge numbers normalized by distance traveled in male pairs of Δ*nvy* (H), pan-neuronal *nvy* RNAi (I), neuron-specific rescue of Δ*nvy* (J), and *nvy* overexpression (K) showed significant changes consistently with their respective phenotypes in raw lunge counts (see Fig. 1 for comparison). *** $p < 0.0005$, * $p < 0.05$, n.s. $p \geq 0.05$ [(A,C,E,F-K), Kruskal–Wallis one-way ANOVA and post-hoc Mann–Whitney U-test with Bonferroni correction.]

Supplemantary Figure S2.

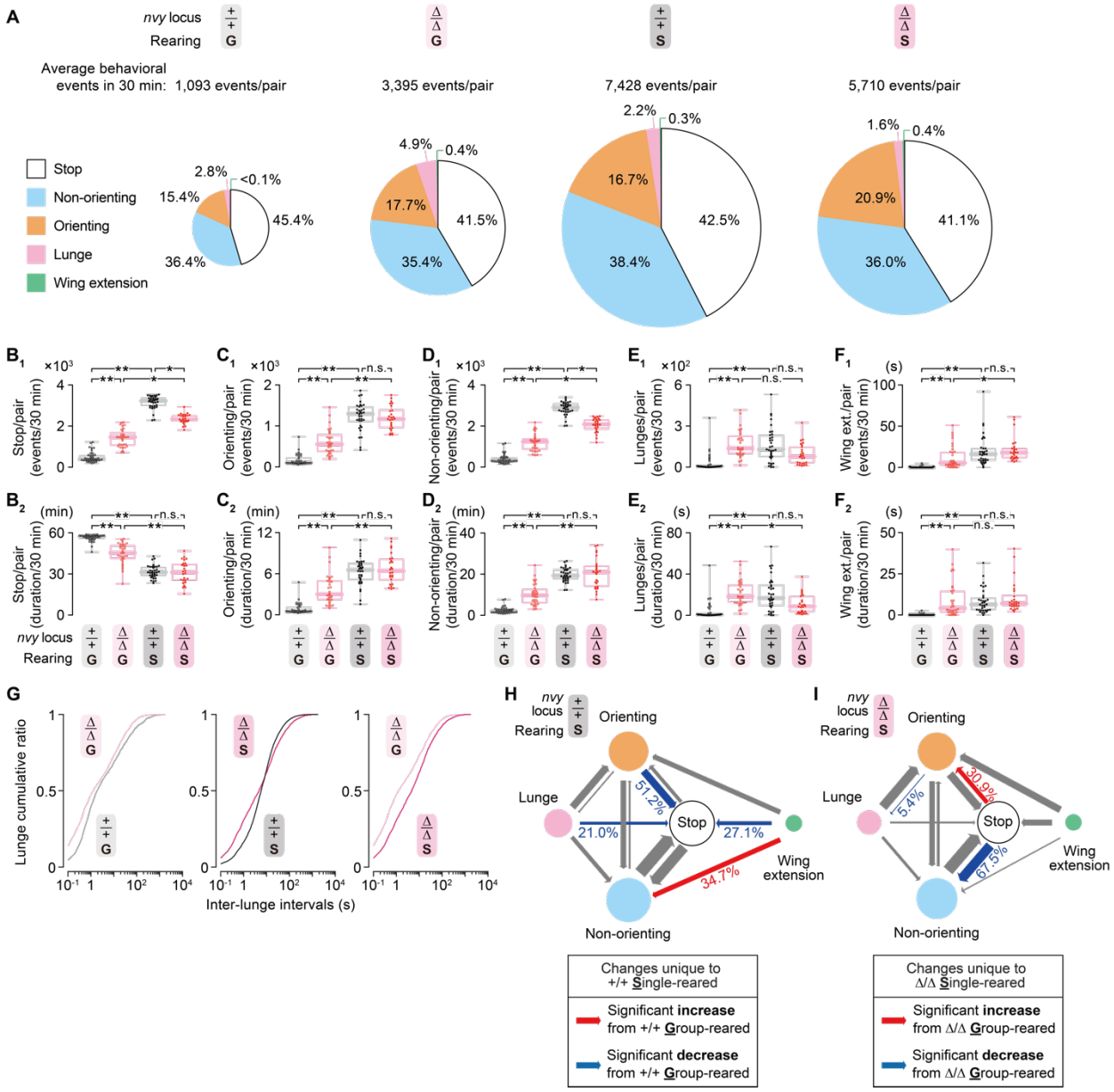

Fig. S2. Additional analysis related to behavioral transitions in wild-type and Δ*nvy* males.
(**A**) Breakdown of 5 classified behaviors performed by (from left) group-reared Δ*nvy* males, group-reared wild type males, single-reared Δ*nvy* males, and single-reared wild-type males. The diameter of pie charts is proportional to the square root of behavioral events per pair. (**B to F**) Quantification of the number (**B_1 to F_1**) and the total duration (**B_2 to F_2**) of stopping (B), orienting (C), non-orienting (D), lunge (E), and wing extension (F) of group-reared wild-type males, group-reared Δ*nvy* males, single-reared wild-type males, and single-reared Δ*nvy* males. Note that the maximum value of "duration/30 min" in B_2–F_2 is 60 minutes per pair to account for the combined values from both flies. (**G**) Cumulative plots of inter-lunge intervals in group-reared wild type males (gray), group-reared Δ*nvy* males (light pink), single-reared wild-type males (black), and single-reared Δ*nvy* males (dark pink). Note that the x-axis (intervals) is scaled

in logarithm. **(H, I)** Ethograms between 5 classified behaviors for single-reared wild-type (H) (replot of Fig. 2C) and single-reared Δ*nvy* (I) males. Numbers represent transition probabilities from the source of arrows. ** $p < 0.005$, * $p < 0.05$, n.s. $p \geq 0.05$ [(B,D,F,G) Kruskal–Wallis one-way ANOVA and post-hoc Mann–Whitney U-test with Bonferroni correction, comparing all combinations]

Supplementary Figure S3.

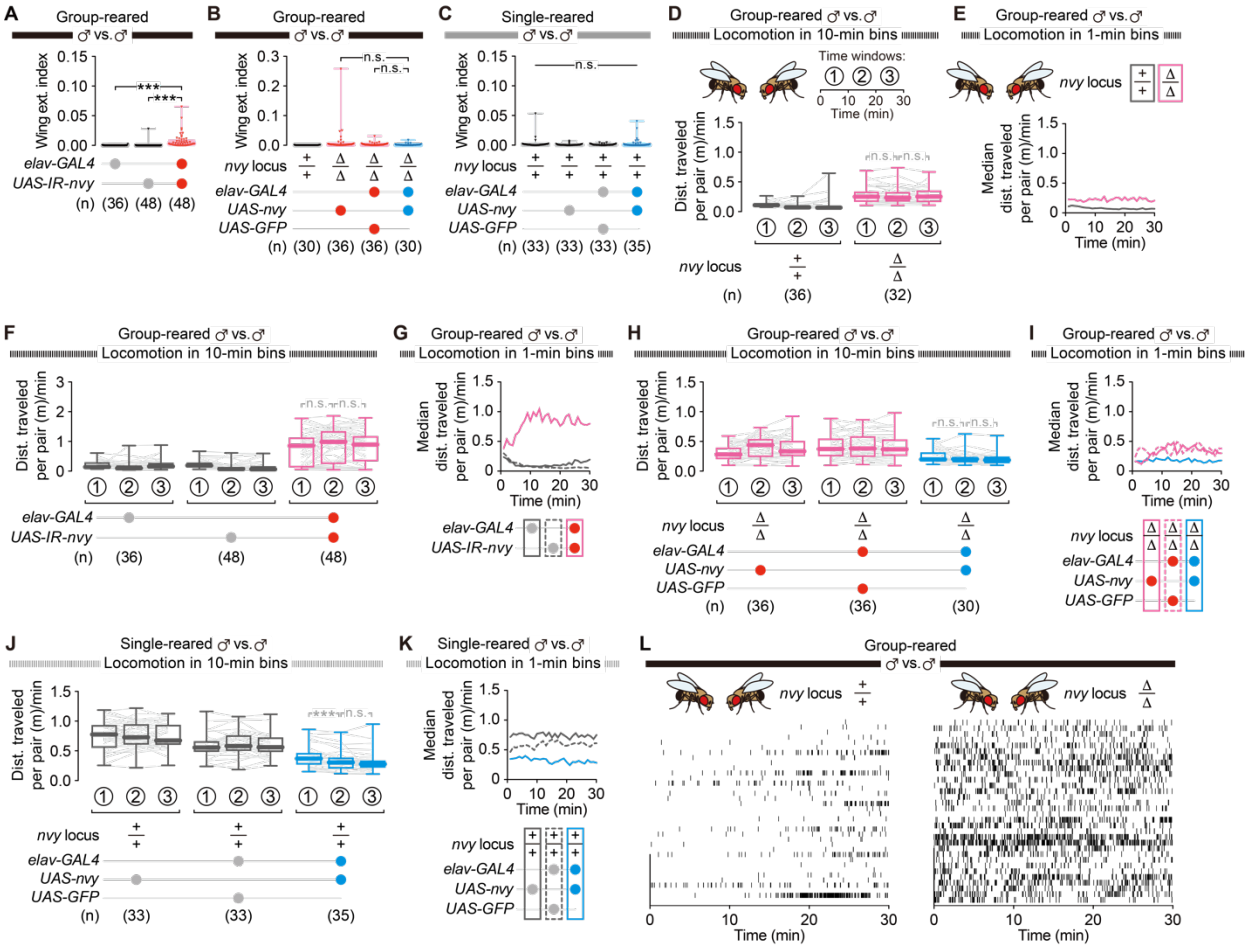

Fig. S3. Temporal dynamics of locomotor and aggressive behaviors in *nvy* mutants.

(**A to C**) Male-to-male wing extensions analyzed from the movies used in Fig. 1. RNAi of *nvy* increased the wing extension duration (A), whereas Δ*nvy* rescue (B) and *nvy* overexpression did not (C). (**D to K**) Temporal changes of locomotor activities in fly pairs during aggression assays in Fig. 1. Locomotion was analyzed in detail for Δ*nvy* mutants (D and E), *nvy* RNAi (F and G), Δ*nvy* rescue (H and I), and *nvy* overexpression (J and K), each in 10-min (D, F, H, J) or 1-min (E, G, I, K) bins. **(L)** Raster plots of lunges performed by either wild-type (left) or Δ*nvy* male pairs shown in Fig. 1D. *** $p < 0.0005$, n.s. $p \geq 0.05$ [(A), (B), (C), in black: Kruskal–Wallis one-way ANOVA and post-hoc Mann–Whitney U-test with Bonferroni correction; (D), (F), (H), (J), in gray: Kruskal–Wallis one-way ANOVA and post-hoc Wilcoxon signed rank test.]

Supplementary Figure S4.

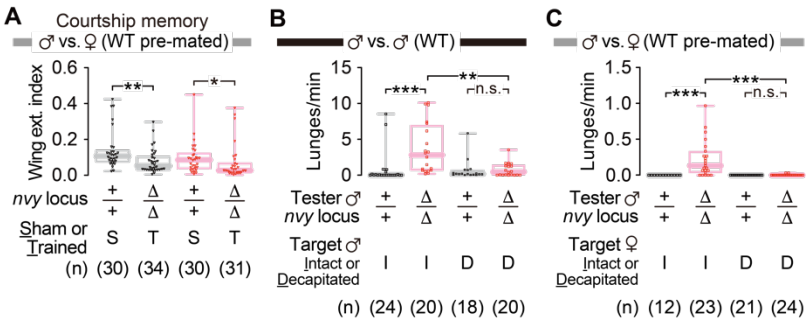

Fig. S4. Additional characterization of the behavior of Δ*nvy* males toward a female

(**A**) Wing extension indices of males during the test session of courtship memory assay. Males were previously either trained with pre-mated females ("T") or sham-trained ("S"). (**B, C**) Aggression by Δ*nvy* males requires behavioral feedback from the opponent. Lunges in 30 min by either wild-type or Δ*nvy* tester males, toward intact ("I") or decapitated ("D") wild-type target males (B) or pre-mated females (C). *** $p < 0.0005$, ** $p < 0.005$, * $p < 0.05$, n.s. $p \geq 0.05$ [(A), (B), (C), Kruskal–Wallis one-way ANOVA and post-hoc Mann–Whitney U-test with Bonferroni correction.]

Supplementary Figure S5.

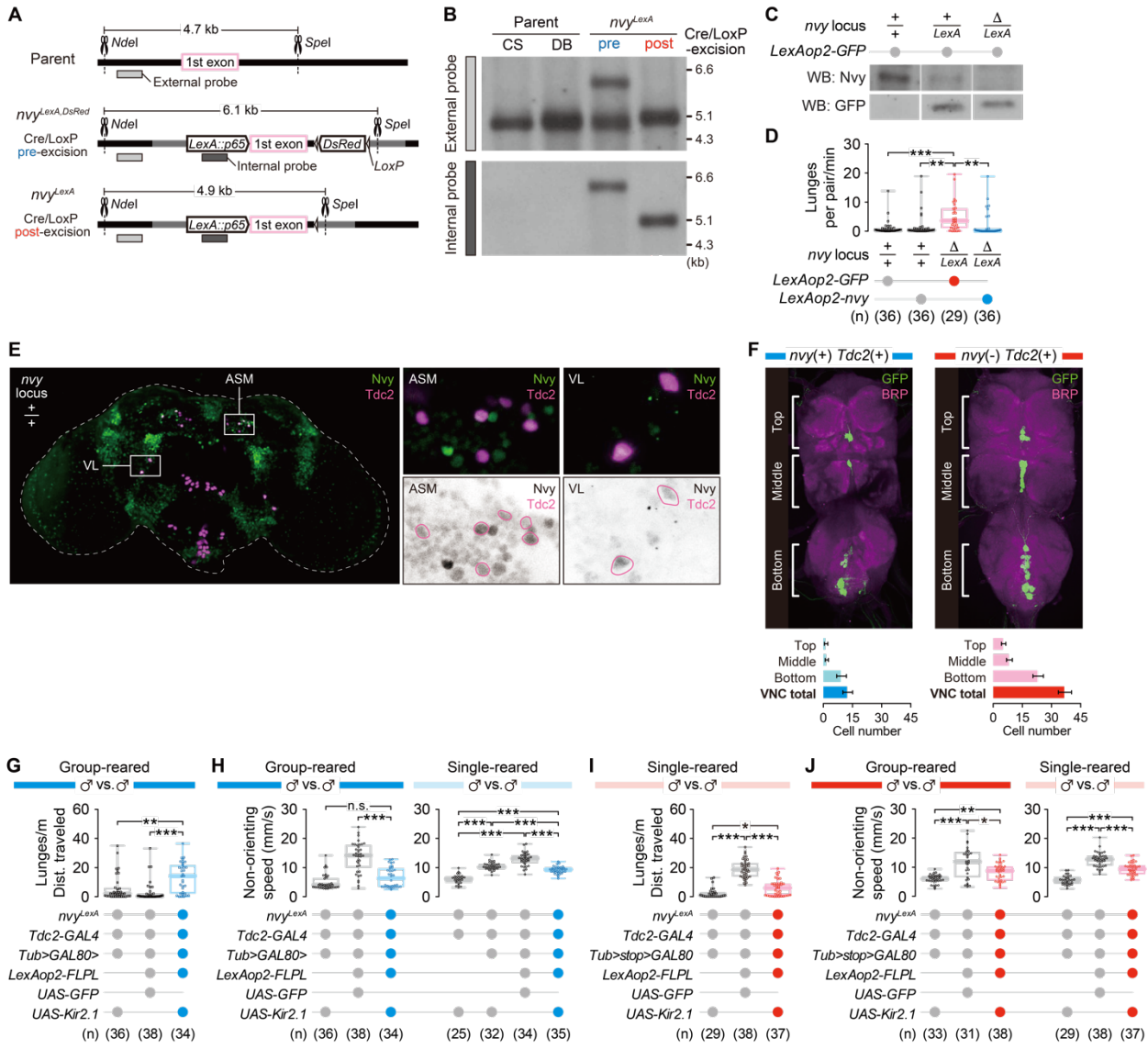

Fig. S5. Generation of the *nvy*^{LexA} knock-in lines, and additional histological/behavioral characterization of *nvy*-expressing neurons.

(**A**) Genome schematics of the *nvy*^{LexA} knock-in alleles. The *nvy* locus of the parental line (top) was targeted by CRISPR/Cas9-mediated cleavage, leading to homologous recombination with the plasmid harboring the coding sequences of *LexA::p65* and the eye-specific genetic marker *3XP3-DsRed* (middle). After backcrossing with the wild-type strain, the *DsRed* marker flanked by *LoxP* was excised by crossing with an *hs-Cre* line (bottom). Predicted distances between the recognition sites of two restriction enzymes, *Nde*I and *Spe*I, are shown for each genotype. For the following Southern blot analysis, one region outside the *nvy* exon and another region inside the *LexA::p65* coding sequence were targeted by "external" and "internal" probes, respectively. (**B**) Southern blot analysis of the parental and *nvy*^{LexA} knock-in lines. *Nde*I/*Spe*I-digested genomic DNA from each line was hybridized with either the external (top) or internal (bottom) probe. For parental lines, the wild-type Canton-S (CS) used for backcrossing and the "double-balancer"

(DB: *w*; *Bl*/*CyO*; *TM2*/*TM6B*) used to establish the knock-in lines are shown. Note that the nvy^{LexA} knock-in lines were maintained with the second chromosome balancer *CyO* derived from the parental DB line. (**C**) Western blot analysis of Nvy protein extracted from the nvy^{LexA} fly heads. (**D**) Hyperaggressive phenotype induced by trans-heterozygosity of nvy^{LexA} and Δ*nvy*, and its rescue by *nvy* expression. (**E**) Immunohistochemistry using anti-Nvy antibody reveals a broad expression pattern in the fly brain with signals colocalized with *Tdc2-GAL4*-driven tdTomato. Representative areas containing two OA/TA subpopulations (ASM and VL) mainly co-labeled by nvy^{LexA} and *Tdc2-GAL4* (see Fig. 4C and 4D) are shown at high magnification. (**F**) GFP expression in *nvy*-positive (left) or *nvy*-negative (right) *Tdc2* neurons in the VNC is visualized by immunohistochemistry. VNC was divided into three regions ("top" being closest to the head) and cell counts for each area were shown as means ± S.D. of 5 brains. (**G to J**) Locomotion changes followed by *Kir2.1*-mediated silencing of *Tdc2* subpopulations, analyzed from the movies used in Fig. 4E and 4G. Changes in lunge numbers normalized by distance traveled in group-reared *nvy*-positive *Tdc2* neurons (G) and single-reared *nvy*-negative *Tdc2* cells (I) were consistent to the raw lunge results shown in Fig. 4. Speed during non-orienting locomotion changed irrespectively to lunge patterns in flies expressing *Kir2.1* in *nvy*-positive *Tdc2* neurons (H), whereas both correlated with each other when *Kir2.1* was expressed in *nvy*-negative *Tdc2* neurons (J). *** $p < 0.0005$, ** $p < 0.005$, * $p < 0.05$, n.s. $p \geq 0.05$ [(D) Kruskal–Wallis one-way ANOVA and post-hoc Mann–Whitney U-test with Bonferroni correction.]

Supplementary Figure S6.

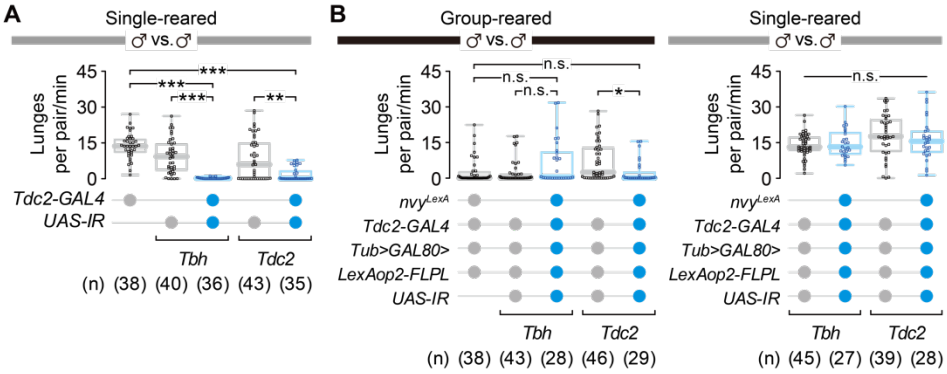

Fig. S6. Knock-down of octopamine/tyramine biosynthesis genes in the *nvy*-positive *Tdc2* neurons.
(**A**) Decrease in lunges by single-reared males after *Tbh* and *Tdc2* RNAi in the entire *Tdc2* neurons. (**B**) Neither RNAi of *Tbh* nor *Tdc2* in the *nvy*-positive *Tdc2* neurons significantly affected aggressiveness of group- (left) or single-reared (right) males. *** $p < 0.0005$, ** $p < 0.005$, * $p < 0.05$, n.s. $p \geq 0.05$ [(A), (B), Kruskal–Wallis one-way ANOVA and post-hoc Mann–Whitney U-test with Bonferroni correction.]

Supplemtary Figure S7.

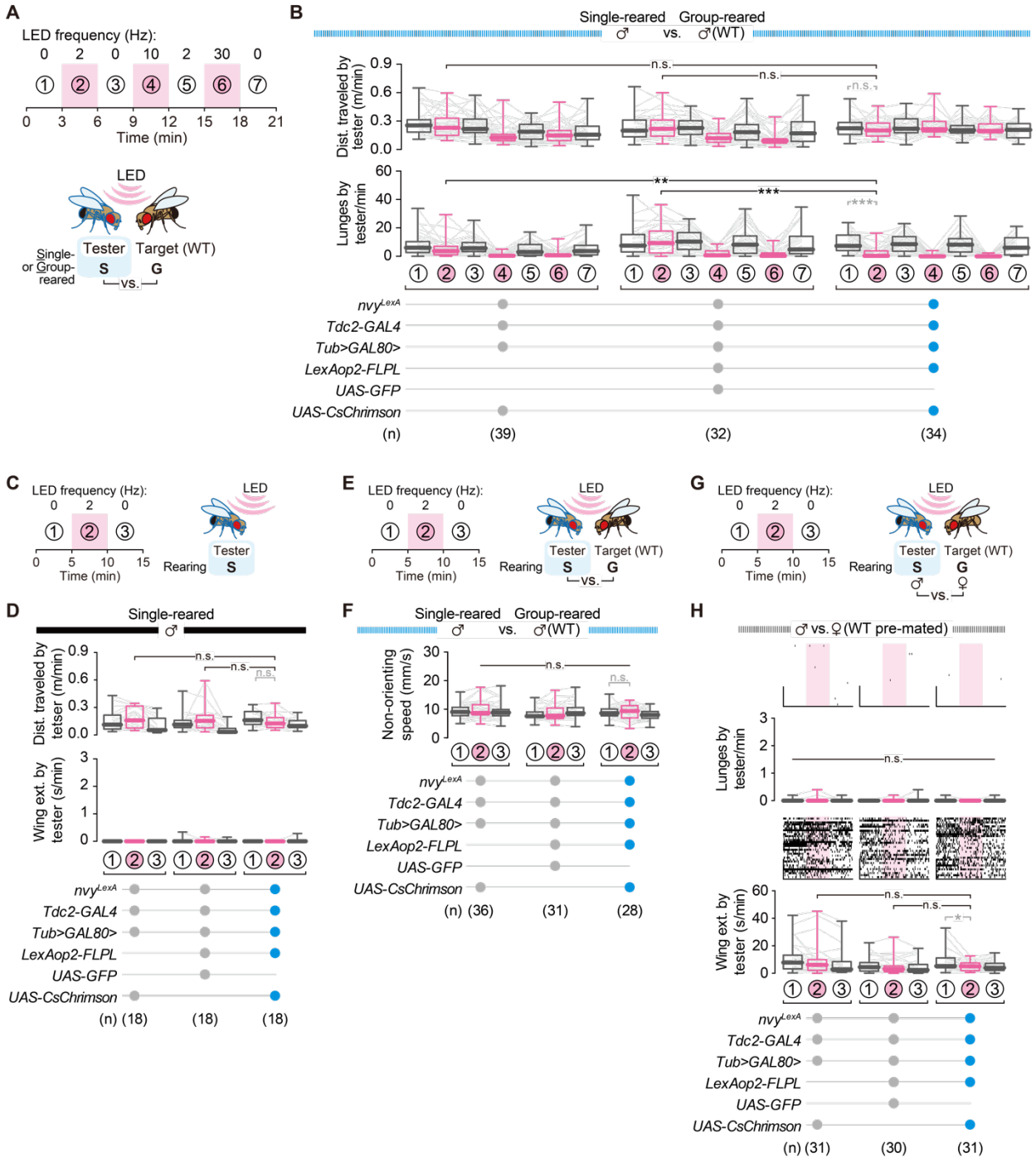

Fig. S7. Additional behavioral data obtained during optogenetic stimulation of *nvy*-positive *Tdc2* neurons.

(**A, B**), Optogenetic stimulation of *nvy*-positive *Tdc2* neurons at various LED frequencies. The stimulation was performed at 2, 10, and 30 Hz for 3 min, each separated by a 3-min interval (A). Distance traveled (B; top) and lunges (B; bottom) performed by tester males during each 3-min time window are shown in box plots. (**C, D**) Optogenetic stimulation of *nvy*-positive *Tdc2*

neurons in solitary testers. Stimulation was performed at 2 Hz for 5 min in the absence of a target fly (C). Distance traveled (D; top) and wing extensions (D; bottom) performed by tester males during each 5-min time window. (**E, F**) Speed of the "non-orienting" locomotion during optogenetic stimulation of *nvy*-positive *Tdc2* neurons. The original movies used in Fig. 4I were reanalyzed. (**G, H**) Male-to-female lunges and wing extensions during optogenetic stimulation of *nvy*-positive *Tdc2* neurons. Male testers were paired with wild-type pre-mated females, and the stimulation was performed at 2 Hz for 5 min (G). Lunges (H, top) and wing extensions (H, bottom) performed by target males during each 5-min window. The pink area within each raster plot indicates the stimulation period (time window "2" in G). *** $p < 0.0005$, ** $p < 0.01$, * $p < 0.05$, n.s. $p \geq 0.05$ [(B), (D), (F), (H), in black: Kruskal–Wallis one-way ANOVA and post-hoc Mann–Whitney U-test with Bonferroni correction; in gray: Kruskal–Wallis one-way ANOVA and post-hoc Wilcoxon signed rank test.]

Supplementary Figure S8.

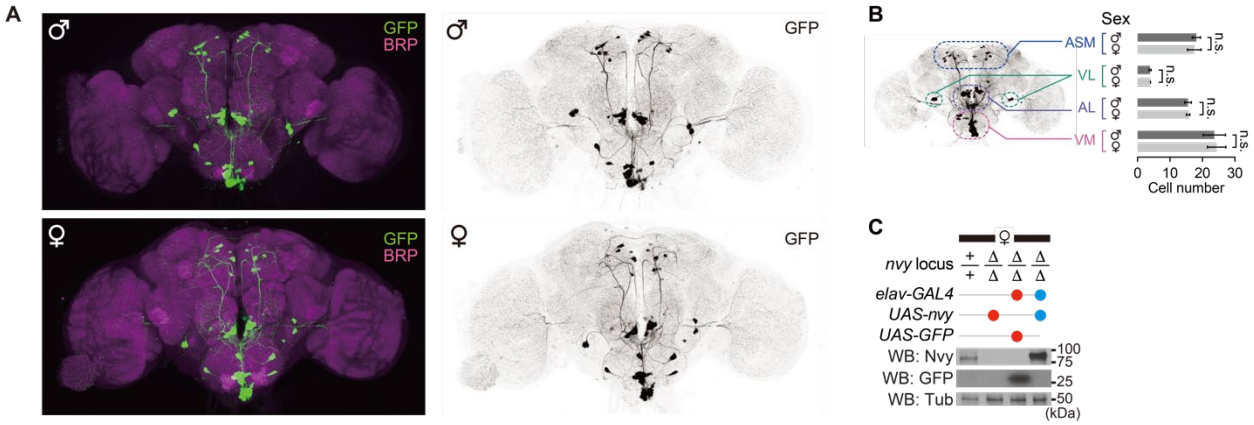

Fig. S8. Gross morphology of *Tdc2* neurons is similar across sexes.

(**A**) Neuronal morphology of *Tdc2* neurons in male and female brains. Left: GFP expressed under the control of *Tdc2-GAL4*, along with the neuropil marker Bruchpilot (BRP), were visualized by immunohistochemistry using male (top) or female (bottom) brains. Right: same images as left with GFP signals visualized in gray scale. (**B**) Cell counts of *Tdc2* neurons in males and females. Subtypes of *Tdc2-GAL4* neurons were classified according to a previous anatomical study (*65*). (**C**) Pan-neuronal expression of Nvy in Δ*nvy* females verified by Western blot. α-Tubulin (Tub) was detected as an internal control. n.s. $p \geq 0.05$ [(B), unpaired t-test; error bars indicate means ± S.D. of 8–9 brains.]

Supplementary Figure S9.

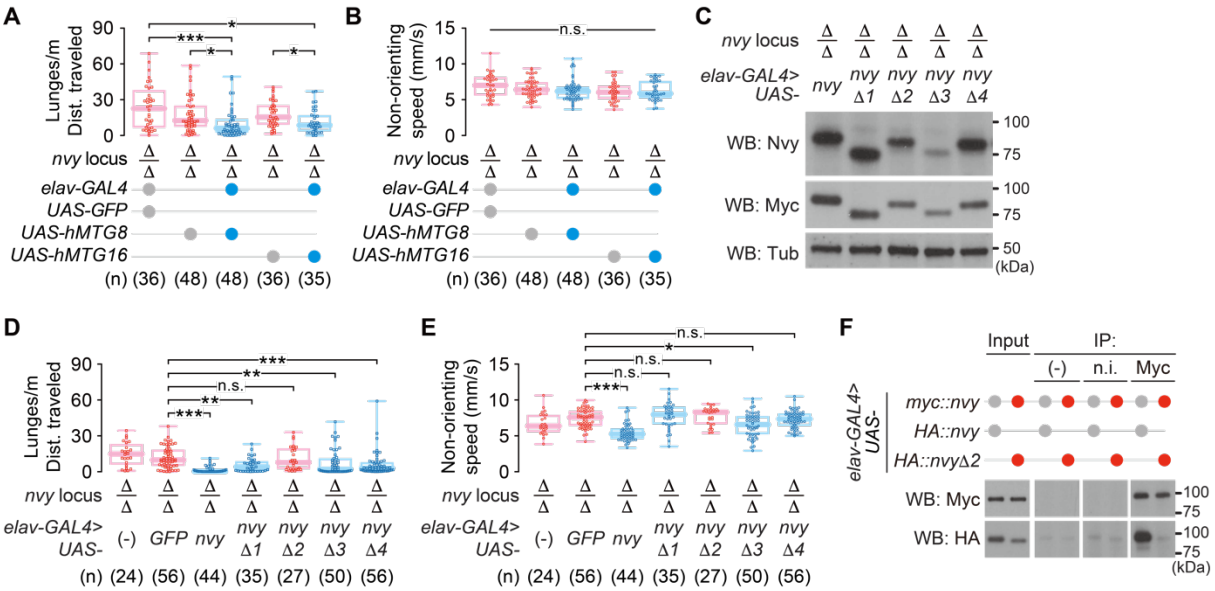

Fig. S9. Additional biochemical and behavioral data for human MTGs and truncated versions of Nvy.

(**A, B**) Locomotion by *MTG*s-expressing male pairs analyzed in Fig. 6C. Pan-neuronal expression of human *MTG*s in the Δ*nvy* background significantly reduced lunge numbers even after normalization by the locomoted distance per pair (B), whereas walking speed during the "non-orienting" state was barely affected (B). (**C**) Pan-neuronal expression of mutated *nvy* transgenes lacking one of the NHR1–4 domains in the Δ*nvy* background. All *UAS-nvy* constructs contain 3xMyc tags at the N-terminus. α-Tubulin (Tub) was used as an internal control. (**D, E**) Locomotion by male pairs expressing truncated *UAS-nvy* constructs analyzed in Fig. 6E. Only *UAS-nvy* lacking the NHR2 domain (*nvyΔ2*) failed to rescue the Δ*nvy* phenotype for lunge numbers normalized by distance traveled per pair (D), which is in agreement with the raw lunge result in Fig. 6E. The *UAS-nvyΔ2* expression did not have a significant impact on the non-orienting walking speed of the same pairs (E). (**F**) Homo-multimer formation of Nvy protein mediated by the NHR2 domain. Myc-tagged Nvy was co-immunoprecipitated with either HA-tagged intact Nvy or the mutated version lacking NHR2. Input: 7.5% of lysate used for the precipitation. IP, (-): samples precipitated with no antibody. IP, n.i.: samples precipitated with normal IgG. IP, Myc: samples precipitated with an anti-Myc antibody. *** $p < 0.0005$, ** $p < 0.005$, * $p < 0.05$, n.s. $p \geq 0.05$ [(A,B,D,E), Kruskal–Wallis one-way ANOVA and post-hoc Mann–Whitney U-test with Bonferroni correction.]

Supplementary Figure S10.

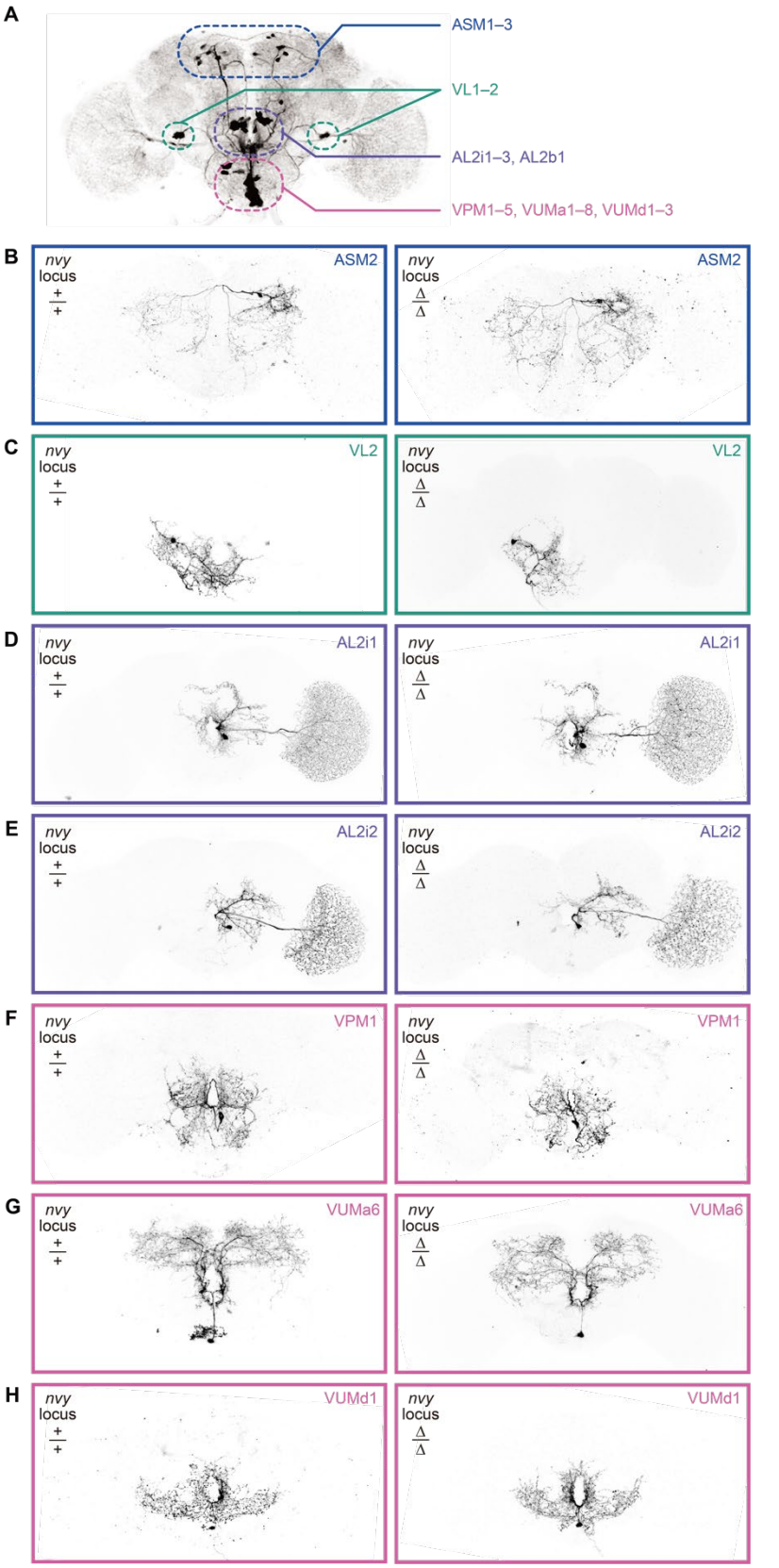

Fig. S10. *Tdc2* neurons in Δ*nvy* males largely retain their anatomical characteristics.
(**A**) Locations of *Tdc2* neuronal clones identified in both wild-type and Δ*nvy* males. Nomenclature is based on (*65*). The image is reproduced from Fig. 4C. (**B** to **H**) Images of single *Tdc2* neuronal clones produced by MultiColor FlpOut, from wild type (left) and Δ*nvy* (right) males. Names of cell types are indicated at the top right corner.

Supplementary Figure S11.

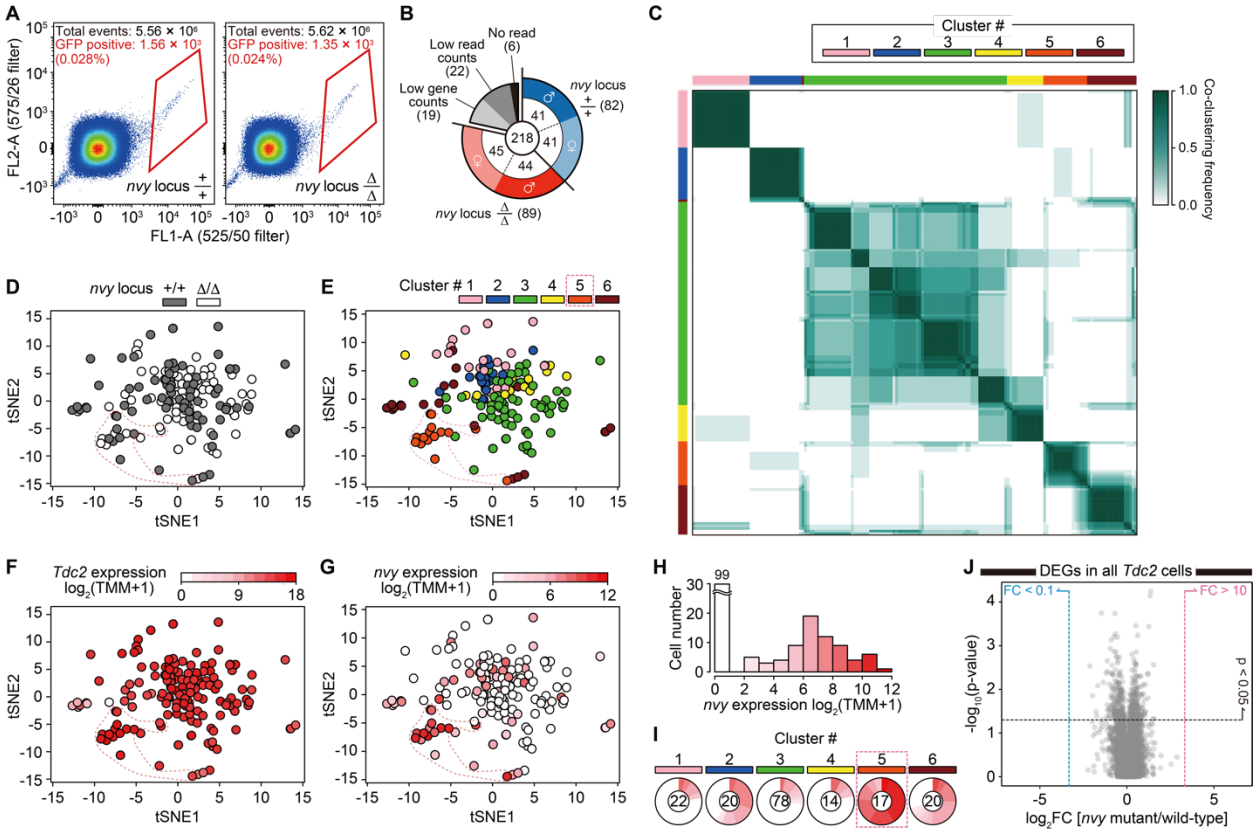

Fig. S11. Additional analyses of cell clusters and DEGs from single-cell RNA-sequencing of *Tdc2* neurons.

(**A**) FACS results for GFP-labeled *Tdc2* cells. GFP-positive cells inside the red lines were collected for sequencing. (**B**) Number of cells used in the sequencing analysis. (**C**) Co-clustering frequency matrix from the iterative clustering analysis with 100 random samplings. The plot shows the probability of co-occurrence in the same cluster for given pairs of cells. (**D** to **G**) tSNE plots of sequenced *Tdc2* cells, color-coded for the *nvy* locus genotypes (D; wild-type in black, Δ*nvy* in white), cell clusters (E), and expression levels of *Tdc2* (F) or *nvy* (G). (**H**) Histogram of *Tdc2* cells according to the expression level of *nvy*. (**I**) Ratio of *nvy*-expressing cells within each cluster. Red intensity corresponds to the level of *nvy* expression shown in G and H. Total cell numbers for each cluster are shown at the center. (**J**) A volcano plot of DEGs analyzed in all *Tdc2* cells. Dots are plotted according to the fold change (FC) and the p-value (by Mann–Whitney U-test) of each gene when the Δ*nvy* mutant cells were compared against the wild-type cells.

Supplementary Figure S12.

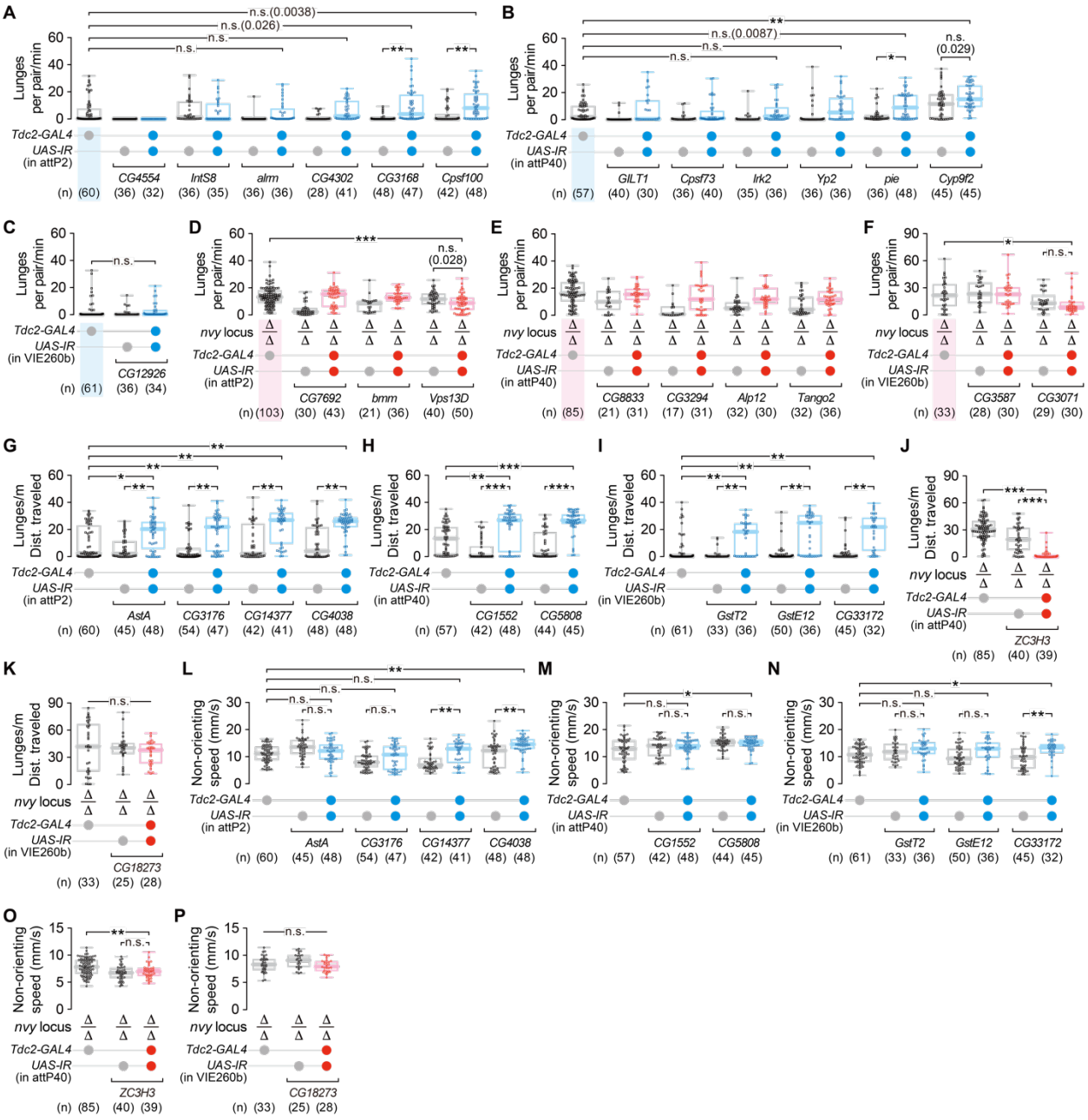

Fig. S12. Additional behavioral data related to RNAi of DEGs in *Tdc2* neurons.

(**A** to **C**) Lunges performed by males with *Tdc2-GAL4* driving RNAi constructs of down-regulated DEGs in cluster #5 that did not elevate aggression compared to at least one genetic control. *UAS-IR* constructs were inserted either in attP2 (A), attP40 (B), or VIE260b (C). (**D** to **F**) Lunges performed by Δ*nvy* males with *Tdc2-GAL4* driving RNAi constructs of up-regulated DEGs in cluster #5 that did not reverse high levels of aggression in the homozygous Δ*nvy* background compared to at least one genetic control. *UAS-IR* constructs were inserted either in attP2 (D), attP40 (E), or VIE260b (F). Colored boxes on the genotypes indicate that the genetic control results (i.e., *Tdc2-GAL4*-only controls with empty vectors inserted in each landing site)

were replotted in Fig. 7 as a part of the same experiment. (**G to K**) Lunge numbers normalized by distance traveled in the male pairs following *Tdc2-GAL4*-driven RNAi against up- (G to I) and down-regulated (J to K) DEGs, of which lunges were analyzed in Fig. 7F–J. Values were mostly consistent with the raw lunge results, except for *CG182723* RNAi in Δ*nvy* background (K). (**L to P**) Locomotion speed during non-orienting by the male pairs analyzed in Fig. 7F–J. *** $p < 0.0005$, ** $p < 0.01$, * $p < 0.05$, n.s. $p \geq 0.05$ [(A) to (P), Kruskal–Wallis one-way ANOVA and post-hoc Mann–Whitney U-test with Bonferroni correction.]

Supplementary Figure S13.

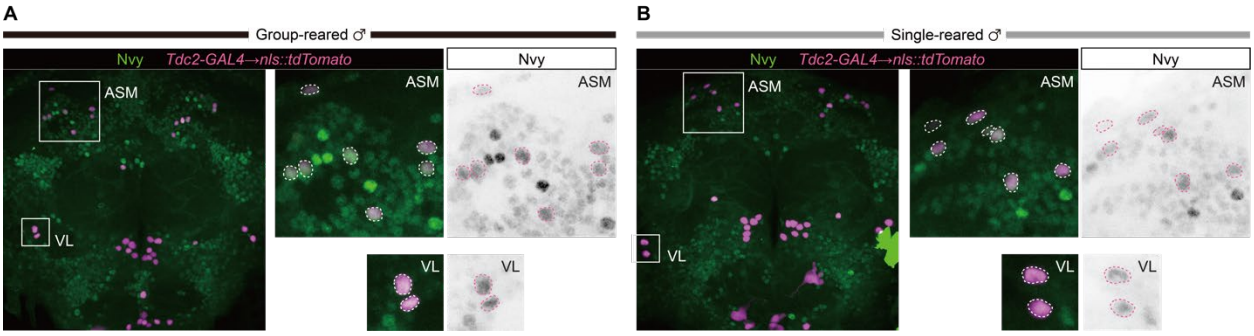

Fig. S13. Additional expression data related to *nvy* functions in *Tdc2* neurons.
Nvy immunoreactivities (green) in ASM and VL clusters of *Tdc2* neurons (labeled by nuclear-localizing tdTomato, magenta) from group-reared (**A**) and single-reared (**B**) male brains.

Table S3. Results of the *nvy*-RNAi GAL4 screen.

Supplementary Table S3. Results of the *nvy*-RNAi GAL4 screen

I. GAL4	II. 25th percentile	III. Median	IV. 75th percentile	V. n	VI. P-value vs GAL4-only control	VII. P-value vs UAS-only control
Tdc2	**12.00**	**363.0**	**844.0**	**35**	**<0.0001 (<0.0002)**	**0.0007 (0.0014)**
Fru	**10.50**	**48.50**	**667.5**	**42**	**<0.0001 (<0.0004)**	**<0.0001 (<0.0004)**
Mip	4.250	42.00	311.8	24	0.9552	0.0043 (0.0344)
Orco	8.750	41.00	731.3	34	0.1368	0.0720
R84H09	**3.000**	**40.00**	**209.8**	**36**	**<0.0001 (<0.0008)**	**0.0002 (0.0016)**
R20G01	4.250	25.50	407.0	36	0.0090 (0.0720)	<0.0001 (<0.0008)
Ey(4-8)	3.000	25.00	319.3	36	0.0344 (0.1376)	0.1892
NP2631	**3.500**	**17.00**	**128.5**	**49**	**<0.0001 (<0.0002)**	**<0.0001 (<0.0002)**
Capa	1.250	15.50	329.8	36	0.2471	0.0326 (0.1956)
GH146	1.250	11.00	46.50	30	0.2280	0.0043 (0.0172)
Npf	1.000	10.00	314.5	46	0.8135	0.0143 (0.0572)
5HTR1B(II)	1.750	9.500	311.3	30	0.0581	0.0006 (0.0024)
Ey(3-8)	1.000	9.500	430.3	36	0.9337	0.9671
Ato(10)	1.000	8.500	40.00	36	0.8730	0.5607
R38G08	2.000	7.500	20.00	22	0.2481	0.0413 (0.2478)
Trh	2.000	7.000	91.75	36	0.6056	0.6070
R93G12	3.000	7.000	18.00	27	0.3155	0.0579
Dsk	1.250	6.000	41.00	24	0.8817	0.1495
Akh	2.000	5.000	10.25	30	0.5929	0.0026 (0.0208)
Eth	1.250	4.500	29.75	36	<0.0001 (<0.0006)	0.1495
Dh31	3.000	4.500	25.00	24	0.9304	0.1990
Pdf	1.250	4.000	20.25	36	0.4062	0.0228 (0.0912)
R27G01	1.000	4.000	6.000	30	0.1254	0.0003 (0.0018)
AstA1	2.250	3.500	9.000	24	0.4076	0.9058
AstC	1.000	3.500	9.250	36	0.7080	0.0407 (0.3256)
Dh44	0.250	3.500	9.750	24	0.8409	0.9712
Burs	1.250	3.000	24.25	24	0.0109 (0.0654)	0.8333
R70B01	1.000	3.000	6.000	30	0.0186 (0.1116)	0.7708
R11H09	1.000	3.000	14.25	30	0.9912	0.5981
Poxn	0.7500	2.500	5.000	30	0.5119	0.7420
Crz	0.7500	2.000	23.75	30	0.9026	0.4760
R17C11	1.000	2.000	6.000	30	0.2980	0.0012 (0.0072)
R15F02	0.0	2.000	4.250	30	0.1968	0.4381
Ppk23	0.0	2.000	8.000	24	0.3787	0.5499
Ddc(II)	0.0	2.000	23.00	23	0.9701	0.4673
AstA2	0.2500	1.500	6.000	24	0.5866	0.4224
FMRFa	0.0	1.000	5.500	24	0.9958	0.0513
Droc	0.0	1.000	6.500	30	0.6060	0.5257
5HTR1B(III)	0.0	1.000	4.250	30	0.9673	0.2972
R16F12	0.0	1.000	6.000	27	0.8409	0.0301 (0.1806)
Ppk25	0.0	1.000	2.750	24	0.0870	0.5398
Dsx	0.0	1.000	3.750	30	0.0009 (0.0036)	0.4744
Amon	0.0	1.000	23.00	24	0.0004 (0.0024)	0.8937
Ddc(III)	0.0	1.000	2.000	24	0.2483	0.4869

Notes:
Group-reared males harboring either *XX-GAL4*, *UAS-IR-nvy*, or both *XX-GAL4* and *UAS-IR-nvy* were paired each with same genotypes. Lunge counts and pair numbers tested for the knockdown mutants are shown in II–V. Statistical significances between the knockdown mutants and two genetic controls were analyzed by Kruskal–Wallis one-way ANOVA and post-hoc Mann–Whitney U-test. P-values between knockdown mutant pairs and GAL4-only (VI) or UAS-only (VII) pairs are shown. Adjusted p-values by Bonferroni correction within each experiment are shown in parenthesis.
Data in bold indicate 4 out of 44 tested *GAL4*s where knockdown mutants showed significant increase in lunges compared to two genetic controls, with corrected p-values less than 0.05.

Table S1. (separate file)
Results of the primary RNAi screen (.xlsx file).

Table S2. (separate file)
Results of the secondary RNAi screen (.xlsx file).

Table S4. (separate file)
The list of the complete genotypes used in this study (.xlsx file).

Table S5. (separate file)
Sequences of primers used in this study (.xlsx file).

Table S6. (separate file)
The list of antibodies, along with concentration and incubation conditions for Western blotting experiments (.xlsx file).

Table S7. (separate file)
Sequences data from scRNAseq experiments (.txt file). Data were filtered and normalized as described in Materials and Methods.

Table S8. (separate file)
The list of software used in this study (.xlsx file).

Movie S1.

An example of interactions between a pair of group-reared wild-type males (a sample from the dataset used in Fig. 1D).

Movie S2.

An example of interactions between a pair of group-reared Δ*nvy* males (a sample from the dataset used in Fig. 1D).

Movie S3.

An example of interactions between a group-reared wild-type male and a pre-mated female (a sample from the dataset used in Fig. 3C).

Movie S4.

An example of interactions between a group-reared Δ*nvy* male and a pre-mated female (a sample from the dataset used in Fig. 3C).

Movie S5.

Three-dimensional rendering of *nvy*-positive *Tdc2* neurons (a sample from Fig. 4D).

Movie S6.

Three-dimensional rendering of *nvy*-negative *Tdc2* neurons (a sample from Fig. 4F).

Movie S7.

An example of interactions between a group-reared wild-type male and a group-reared male in which CsChrimson was expressed in *nvy*-positive *Tdc2* neurons, before and during the LED stimulation (a sample from the dataset used in Fig. 4I).

Movie S8.

An example of interactions between a group-reared wild-type male and a male from one of genetic controls (which lacks *LexAop2-FLP*) of the optogenetic experiment in Fig. 4I, before and during the LED stimulation.

Movie S9.

Three-dimensional rendering of *Tdc2* neurons in a wild-type male (a sample from Fig. 7A).

Movie S10.

Three-dimensional rendering of *Tdc2* neurons in a Δ*nvy* male (a sample from Fig. 7A).

Data S1. (separate file)

The complete statistical results for all applicable figures, and coding sequences of DNA constructs created in this study.

Data S2. (separate file)

Custom R codes for scRNAseq data analysis.

REFERENCES AND NOTES

1. J. M. Smith, *Evolution and the Theory of Games* (Cambridge Univ. Press, 1982).

2. H. A. Dierick, R. J. Greenspan, Molecular analysis of flies selected for aggressive behavior. *Nat. Genet.* **38**, 1023–1031 (2006).

3. J. Shorter, C. Couch, W. Huang, M. A. Carbone, J. Peiffer, R. R. H. Anholt, T. F. C. Mackay, Genetic architecture of natural variation in *Drosophila melanogaster* aggressive behavior. *Proc. Natl. Acad. Sci. U.S.A.* **112**, E3555–E3563 (2015).

4. S. A. Golden, M. Heshmati, M. Flanigan, D. J. Christoffel, K. Guise, M. L. Pfau, H. Aleyasin, C. Menard, H. Zhang, G. E. Hodes, D. Bregman, L. Khibnik, J. Tai, N. Rebusi, B. Krawitz, D. Chaudhury, J. J. Walsh, M.-H. Han, M. L. Shapiro, S. J. Russo, Basal forebrain projections to the lateral habenula modulate aggression reward. *Nature* **534**, 688–692 (2016).

5. M. Briffa, L. U. Sneddon, A. J. Wilson, Animal personality as a cause and consequence of contest behaviour. *Biol. Lett.* **11**, 20141007 (2015).

6. Y. Hsu, R. L. Earley, L. L. Wolf, Modulation of aggressive behaviour by fighting experience: Mechanisms and contest outcomes. *Biol. Rev. Camb. Philos. Soc.* **81**, 33–74 (2006).

7. L. Wang, H. Dankert, P. Perona, D. J. Anderson, A common genetic target for environmental and heritable influences on aggressiveness in *Drosophila*. *Proc. Natl. Acad. Sci. U.S.A.* **105**, 5657–5663 (2008).

8. J. K. Penn, M. F. Zito, E. A. Kravitz, A single social defeat reduces aggression in a highly aggressive strain of *Drosophila*. *Proc. Natl. Acad. Sci. U.S.A.* **107**, 12682–12686 (2010).

9. A. A. Hoffmann, Z. Cacoyianni, Territoriality in *Drosophila melanogaster* as a conditional strategy. *Anim. Behav.* **40**, 526–537 (1990).

10. J. P. Scott, E. Fredericson, The causes of fighting in mice and rats. *Physiol. Zool.* **24**, 273–309 (1951).

11. V. Diaz, D. Lin, Neural circuits for coping with social defeat. *Curr. Opin. Neurobiol.* **60**, 99–107 (2020).

12. D. An, W. Chen, D.-Q. Yu, S.-W. Wang, W.-Z. Yu, H. Xu, D.-M. Wang, D. Zhao, Y.-P. Sun, J.-C. Wu, Y.-Y. Tang, S.-M. Yin, Effects of social isolation, re-socialization and age on cognitive and aggressive behaviors of Kunming mice and BALB/c mice. *Anim. Sci. J.* **88**, 798–806 (2017).

13. K. J. Flannelly, R. J. Blanchard, M. Y. Muraoka, L. Flannelly, Copulation increases offensive attack in male rats. *Physiol. Behav.* **29**, 381–385 (1982).

14. Q. Yuan, Y. Song, C.-H. Yang, L. Y. Jan, Y. N. Jan, Female contact modulates male aggression via a sexually dimorphic GABAergic circuit in *Drosophila*. *Nat. Neurosci.* **17**, 81–88 (2014).

15. J. T. Cacioppo, L. C. Hawkley, Perceived social isolation and cognition. *Trends Cogn. Sci.* **13**, 447–454 (2009).

16. J. B. Saltz, Genetic variation in social environment construction influences the development of aggressive behavior in *Drosophila melanogaster*. *Heredity (Edinb)* **118**, 340–347 (2017).

17. R. J. Kilgour, A. G. McAdam, G. S. Betini, D. R. Norris, Experimental evidence that density mediates negative frequency-dependent selection on aggression. *J. Anim. Ecol.* **87**, 1091–1101 (2018).

18. P. Ramdya, J. Schneider, J. D. Levine, The neurogenetics of group behavior in *Drosophila melanogaster*. *J. Exp. Biol.* **220**, 35–41 (2017).

19. J. M. Smith, G. R. Price, The logic of animal conflict. *Nature* **246**, 15–18 (1973).

20. R. J. Knell, Population density and the evolution of male aggression. *J. Zool.* **278**, 83–90 (2009).

21. K. Asahina, Neuromodulation and strategic action choice in *Drosophila* aggression. *Annu. Rev. Neurosci.* **40**, 51–75 (2017).

22. E. D. Hoopfer, Neural control of aggression in *Drosophila*. *Curr. Opin. Neurobiol.* **38**, 109–118 (2016).

23. J. E. Lischinsky, D. Lin, Neural mechanisms of aggression across species. *Nat. Neurosci.* **23**, 1317–1328 (2020).

24. P. Chen, W. Hong, Neural circuit mechanisms of social behavior. *Neuron* **98**, 16–30 (2018).

25. F. Wang, J. Zhu, H. Zhu, Q. Zhang, Z. Lin, H. Hu, Bidirectional control of social hierarchy by synaptic efficacy in medial prefrontal cortex. *Science* **334**, 693–697 (2011).

26. M.-Y. Chou, R. Amo, M. Kinoshita, B.-W. Cherng, H. Shimazaki, M. Agetsuma, T. Shiraki, T. Aoki, M. Takahoko, M. Yamazaki, S. Higashijima, H. Okamoto, Social conflict resolution regulated by two dorsal habenular subregions in zebrafish. *Science* **352**, 87–90 (2016).

27. J. Rillich, P. A. Stevenson, A fighter's comeback: Dopamine is necessary for recovery of aggression after social defeat in crickets. *Horm. Behav.* **66**, 696–704 (2014).

28. A. C. Nelson, V. Kapoor, E. Vaughn, J. A. Gnanasegaram, N. D. Rubinstein, V. N. Murthy, C. Dulac, Molecular and circuit architecture of social hierarchy. bioRxiv 838664 (2019).

29. H. A. Dierick, R. J. Greenspan, Serotonin and neuropeptide F have opposite modulatory effects on fly aggression. *Nat. Genet.* **39**, 678–682 (2007).

30. O. Cases, I. Seif, J. Grimsby, P. Gaspar, K. Chen, S. Pournin, U. Muller, M. Aguet, C. Babinet, J. C. Shih, E. De Maeyer, Aggressive behavior and altered amounts of brain serotonin and norepinephrine in mice lacking MAOA. *Science* **268**, 1763–1766 (1995).

31. Z. Wu, A. E. Autry, J. F. Bergan, M. Watabe-Uchida, C. G. Dulac, Galanin neurons in the medial preoptic area govern parental behaviour. *Nature* **509**, 325–330 (2014).

32. M. S. Kayser, B. Mainwaring, Z. Yue, A. Sehgal, Sleep deprivation suppresses aggression in *Drosophila*. *eLife* **4**, e07643 (2015).

33. W. Liu, X. Liang, J. Gong, Z. Yang, Y.-H. Zhang, J.-X. Zhang, Y. Rao, Social regulation of aggression by pheromonal activation of Or65a olfactory neurons in *Drosophila*. *Nat. Neurosci.* **14**, 896–902 (2011).

34. M. Ramin, C. Domocos, D. Slawaska-Eng, Y. Rao, Aggression and social experience: Genetic analysis of visual circuit activity in the control of aggressiveness in *Drosophila*. *Mol. Brain* **7**, 55 (2014).

35. J. M. Donlea, N. Ramanan, P. J. Shaw, Use-dependent plasticity in clock neurons regulates sleep need in *Drosophila*. *Science* **324**, 105–108 (2009).

36. M. Eddison, A genetic screen for *Drosophila* social isolation mutants and analysis of *sex pistol*. *Sci. Rep.* **11**, 17395 (2021).

37. P. Agrawal, D. Kao, P. Chung, L. L. Looger, The neuropeptide Drosulfakinin regulates social isolation-induced aggression in *Drosophila*. *J. Exp. Biol.* **223**, jeb207407 (2020).

38. W. Li, Z. Wang, S. Syed, C. Lyu, S. Lincoln, J. O'Neil, A. D. Nguyen, I. Feng, M. W. Young, Chronic social isolation signals starvation and reduces sleep in *Drosophila*. *Nature* **597**, 239–244 (2021).

39. M. Eddison, D. J. Guarnieri, L. Cheng, C.-H. Liu, K. G. Moffat, G. Davis, U. Heberlein, *arouser* reveals a role for synapse number in the regulation of ethanol sensitivity. *Neuron* **70**, 979–990 (2011).

40. S. C. Hoyer, A. Eckart, A. Herrel, T. Zars, S. A. Fischer, S. L. Hardie, M. Heisenberg, Octopamine in male aggression of *Drosophila*. *Curr. Biol.* **18**, 159–167 (2008).

41. C. Zhou, Y. Rao, Y. Rao, A subset of octopaminergic neurons are important for *Drosophila* aggression. *Nat. Neurosci.* **11**, 1059–1067 (2008).

42. K. Watanabe, H. Chiu, B. D. Pfeiffer, A. M. Wong, E. D. Hoopfer, G. M. Rubin, D. J. Anderson, A circuit node that integrates convergent input from neuromodulatory and social behavior-promoting neurons to control aggression in *Drosophila*. *Neuron* **95**, 1112–1128.e7 (2017).

43. L. M. Sherer, E. Catudio Garrett, H. R. Morgan, E. D. Brewer, L. A. Sirrs, H. K. Shearin, J. L. Williams, B. D. McCabe, R. S. Stowers, S. J. Certel, Octopamine neuron dependent aggression requires dVGLUT from dual-transmitting neurons. *PLOS Genet.* **16**, e1008609 (2020).

44. J. C. Andrews, M. P. Fernandez, Q. Yu, G. P. Leary, A. K. Leung, M. P. Kavanaugh, E. A. Kravitz, S. J. Certel, Octopamine neuromodulation regulates Gr32a-linked aggression and courtship pathways in *Drosophila* males. *PLOS Genet.* **10**, e1004356 (2014).

45. H. Dankert, L. Wang, E. D. Hoopfer, D. J. Anderson, P. Perona, Automated monitoring and analysis of social behavior in *Drosophila*. *Nat. Methods* **6**, 297–303 (2009).

46. X. Leng, M. Wohl, K. Ishii, P. Nayak, K. Asahina, Quantifying influence of human choice on the automated detection of *Drosophila* behavior by a supervised machine learning algorithm. *PLOS ONE* **15**, e0241696 (2020).

47. M. A. Dow, F. von Schilcher, Aggression and mating success in *Drosophila melanogaster*. *Nature* **254**, 511–512 (1975).

48. S. Chen, A. Y. Lee, N. M. Bowens, R. Huber, E. A. Kravitz, Fighting fruit flies: A model system for the study of aggression. *Proc. Natl. Acad. Sci. U.S.A.* **99**, 5664–5668 (2002).

49. H. Chiu, E. D. Hoopfer, M. L. Coughlan, H. J. Pavlou, S. F. Goodwin, D. J. Anderson, A circuit logic for sexually shared and dimorphic aggressive behaviors in *Drosophila*. *Cell* **184**, 507–520.e16 (2021).

50. J. C. Hall, The mating of a fly. *Science* **264**, 1702–1714 (1994).

51. D. Yamamoto, M. Koganezawa, Genes and circuits of courtship behaviour in *Drosophila* males. *Nat. Rev. Neurosci.* **14**, 681–692 (2013).

52. A. J. Calhoun, J. W. Pillow, M. Murthy, Unsupervised identification of the internal states that shape natural behavior. *Nat. Neurosci.* **22**, 2040–2049 (2019).

53. J. C. Hall, Courtship among males due to a male-sterile mutation in *Drosophila melanogaster*. *Behav. Genet.* **8**, 125–141 (1978).

54. R. Thistle, P. Cameron, A. Ghorayshi, L. Dennison, K. Scott, Contact chemoreceptors mediate male-male repulsion and male-female attraction during *Drosophila* courtship. *Cell* **149**, 1140–1151 (2012).

55. N. Svetec, J.-F. Ferveur, Social experience and pheromonal perception can change male-male interactions in *Drosophila melanogaster*. *J. Exp. Biol.* **208**, 891–898 (2005).

56. E. Eyjolfsdottir, S. Branson, X. P. Burgos-Artizzu, E. D. Hoopfer, J. Schor, D. J. Anderson, P. Perona, Detecting social actions of fruit flies. *Computer Vision – ECCV* **8690**, 772–787 (2014).

57. R. Cook, The courtship tracking of *Drosophila melanogaster*. *Biol. Cybern.* **34**, 91–106 (1979).

58. I. M. A. Ribeiro, M. Drews, A. Bahl, C. Machacek, A. Borst, B. J. Dickson, Visual projection neurons mediating directed courtship in *Drosophila*. *Cell* **174**, 607–621.e18 (2018).

59. S. Kohatsu, D. Yamamoto, Visually induced initiation of *Drosophila* innate courtship-like following pursuit is mediated by central excitatory state. *Nat. Commun.* **6**, 6457 (2015).

60. S. P. Nilsen, Y.-B. Chan, R. Huber, E. A. Kravitz, Gender-selective patterns of aggressive behavior in *Drosophila melanogaster*. *Proc. Natl. Acad. Sci. U.S.A.* **101**, 12342–12347 (2004).

61. L. Wang, D. J. Anderson, Identification of an aggression-promoting pheromone and its receptor neurons in *Drosophila*. *Nature* **463**, 227–231 (2010).

62. A. Kurtovic, A. Widmer, B. J. Dickson, A single class of olfactory neurons mediates behavioural responses to a *Drosophila* sex pheromone. *Nature* **446**, 542–546 (2007).

63. H.-H. Lin, D.-S. Cao, S. Sethi, Z. Zeng, J. S. R. Chin, T. S. Chakraborty, A. K. Shepherd, C. A. Nguyen, J. Y. Yew, C.-Y. Su, J. W. Wang, Hormonal modulation of pheromone detection enhances male courtship success. *Neuron* **90**, 1272–1285 (2016).

64. S. H. Cole, G. E. Carney, C. A. McClung, S. S. Willard, B. J. Taylor, J. Hirsh, Two functional but noncomplementing *Drosophila* tyrosine decarboxylase genes: Distinct roles for neural tyramine and octopamine in female fertility. *J. Biol. Chem.* **280**, 14948–14955 (2005).

65. S. Busch, M. Selcho, K. Ito, H. Tanimoto, A map of octopaminergic neurons in the *Drosophila* brain. *J. Comp. Neurol.* **513**, 643–667 (2009).

66. J. Wildonger, R. S. Mann, Evidence that *nervy*, the *Drosophila* homolog of ETO/MTG8, promotes mechanosensory organ development by enhancing Notch signaling. *Dev. Biol.* **286**, 507–520 (2005).

67. M. Selcho, D. Pauls, B. El Jundi, R. F. Stocker, A. S. Thum, The role of octopamine and tyramine in *Drosophila* larval locomotion. *J. Comp. Neurol.* **520**, 3764–3785 (2012).

68. M. E. Flanigan, H. Aleyasin, L. Li, C. J. Burnett, K. L. Chan, K. B. LeClair, E. K. Lucas, B. Matikainen-Ankney, R. Durand-de Cuttoli, A. Takahashi, C. Menard, M. L. Pfau, S. A. Golden, S. Bouchard, E. S. Calipari, E. J. Nestler, R. J. DiLeone, A. Yamanaka, G. W. Huntley, R. L. Clem, S. J. Russo, Orexin signaling in GABAergic lateral habenula neurons modulates aggressive behavior in male mice. *Nat. Neurosci.* **23**, 638–650 (2020).

69. A. Ueda, Y. Kidokoro, Aggressive behaviours of female *Drosophila melanogaster* are influenced by their social experience and food resources. *Physiol. Entomol.* **27**, 21–28 (2002).

70. S. J. Certel, A. Leung, C.-Y. Lin, P. Perez, A.-S. Chiang, E. A. Kravitz, Octopamine neuromodulatory effects on a social behavior decision-making network in *Drosophila* males. *PLOS ONE* **5**, e13248 (2010).

71. M. Koganezawa, K. Kimura, D. Yamamoto, The neural circuitry that functions as a switch for courtship versus aggression in *Drosophila* males. *Curr. Biol.* **26**, 1395–1403 (2016).

72. H. Lee, D.-W. Kim, R. Remedios, T. E. Anthony, A. Chang, L. Madisen, H. Zeng, D. J. Anderson, Scalable control of mounting and attack by $Esr1^{+}$ neurons in the ventromedial hypothalamus. *Nature* **509**, 627–632 (2014).

73. K. Hashikawa, Y. Hashikawa, R. Tremblay, J. Zhang, J. E. Feng, A. Sabol, W. T. Piper, H. Lee, B. Rudy, D. Lin, $Esr1^{+}$ cells in the ventromedial hypothalamus control female aggression. *Nat. Neurosci.* **20**, 1580–1590 (2017).

74. E. K. Unger, K. J. Burke Jr., C. F. Yang, K. J. Bender, P. M. Fuller, N. M. Shah, Medial amygdalar aromatase neurons regulate aggression in both sexes. *Cell Rep.* **10**, 453–462 (2015).

75. J. Wang, T. Hoshino, R. L. Redner, S. Kajigaya, J. M. Liu, ETO, fusion partner in t(8;21) acute myeloid leukemia, represses transcription by interaction with the human N-CoR/mSin3/HDAC1 complex. *Proc. Natl. Acad. Sci. U.S.A.* **95**, 10860–10865 (1998).

76. B. Lutterbach, J. J. Westendorf, B. Linggi, A. Patten, M. Moniwa, J. R. Davie, K. D. Huynh, V. J. Bardwell, R. M. Lavinsky, M. G. Rosenfeld, C. Glass, E. Seto, S. W. Hiebert, ETO, a target of t(8;21) in acute leukemia, interacts with the N-CoR and mSin3 corepressors. *Mol. Cell. Biol.* **18**, 7176–7184 (1998).

77. P. G. Feinstein, K. Kornfeld, D. S. Hogness, R. S. Mann, Identification of homeotic target genes in *Drosophila melanogaster* including *nervy*, a proto-oncogene homologue. *Genetics* **140**, 573–586 (1995).

78. J. Wildonger, R. S. Mann, The t(8;21) translocation converts AML1 into a constitutive transcriptional repressor. *Development* **132**, 2263–2272 (2005).

79. J. N. Davis, L. McGhee, S. Meyers, The ETO (MTG8) gene family. *Gene* **303**, 1–10 (2003).

80. J. Zhang, B. A. Hug, E. Y. Huang, C. W. Chen, V. Gelmetti, M. Maccarana, S. Minucci, P. G. Pelicci, M. A. Lazar, Oligomerization of ETO is obligatory for corepressor interaction. *Mol. Cell. Biol.* **21**, 156–163 (2001).

81. Y. Liu, M. D. Cheney, J. J. Gaudet, M. Chruszcz, S. M. Lukasik, D. Sugiyama, J. Lary, J. Cole, Z. Dauter, W. Minor, N. A. Speck, J. H. Bushweller, The tetramer structure of the Nervy homology two domain, NHR2, is critical for AML1/ETO's activity. *Cancer Cell* **9**, 249–260 (2006).

82. B. Tasic, Z. Yao, L. T. Graybuck, K. A. Smith, T. N. Nguyen, D. Bertagnolli, J. Goldy, E. Garren, M. N. Economo, S. Viswanathan, O. Penn, T. Bakken, V. Menon, J. Miller, O. Fong, K. E. Hirokawa, K. Lathia, C. Rimorin, M. Tieu, R. Larsen, T. Casper, E. Barkan, M. Kroll, S. Parry, N. V. Shapovalova, D. Hirschstein, J. Pendergraft, H. A. Sullivan, T. K. Kim, A. Szafer, N. Dee, P. Groblewski, I. Wickersham, A. Cetin, J. A. Harris, B. P. Levi, S. M. Sunkin, L. Madisen, T. L.

Daigle, L. Looger, A. Bernard, J. Phillips, E. Lein, M. Hawrylycz, K. Svoboda, A. R. Jones, C. Koch, H. Zeng, Shared and distinct transcriptomic cell types across neocortical areas. *Nature* **563**, 72–78 (2018).

83. R. J. Nelson, S. Chiavegatto, Aggression in knockout mice. *ILAR J.* **41**, 153–162 (2000).

84. F. Wu, B. Deng, N. Xiao, T. Wang, Y. Li, R. Wang, K. Shi, D.-G. Luo, Y. Rao, C. Zhou, A neuropeptide regulates fighting behavior in *Drosophila melanogaster*. *eLife* **9**, e54229 (2020).

85. S. M. Davis, A. L. Thomas, K. J. Nomie, L. Huang, H. A. Dierick, Tailless and atrophin control *Drosophila* aggression by regulating neuropeptide signalling in the *pars intercerebralis*. *Nat. Commun.* **5**, 3177 (2014).

86. B. A. Hug, M. A. Lazar, ETO interacting proteins. *Oncogene* **23**, 4270–4274 (2004).

87. M. A. Fischer, I. Moreno-Miralles, A. Hunt, B. J. Chyla, S. W. Hiebert, Myeloid translocation gene 16 is required for maintenance of haematopoietic stem cell quiescence. *EMBO J.* **31**, 1494–1505 (2012).

88. J. R. Terman, A. L. Kolodkin, Nervy links protein kinase a to plexin-mediated semaphorin repulsion. *Science* **303**, 1204–1207 (2004).

89. R. J. Ice, J. Wildonger, R. S. Mann, S. W. Hiebert, Comment on "Nervy links protein kinase a to plexin-mediated semaphorin repulsion". *Science* **309**, 558 (2005).

90. J. R. Terman, A. L. Kolodkin, Response to comment on "Nervy links protein kinase a to plexin-mediated semaphorin repulsion". *Science* **309**, 558 (2005).

91. C. E. Holt, K. C. Martin, E. M. Schuman, Local translation in neurons: Visualization and function. *Nat. Struct. Mol. Biol.* **26**, 557–566 (2019).

92. N. Koyano-Nakagawa, C. Kintner, The expression and function of MTG/ETO family proteins during neurogenesis. *Dev. Biol.* **278**, 22–34 (2005).

93. K. Yoon, N. Gaiano, Notch signaling in the mammalian central nervous system: Insights from mouse mutants. *Nat. Neurosci.* **8**, 709–715 (2005).

94. N. C. Inestrosa, E. Arenas, Emerging roles of Wnts in the adult nervous system. *Nat. Rev. Neurosci.* **11**, 77–86 (2010).

95. C. J. Burke, W. Huetteroth, D. Owald, E. Perisse, M. J. Krashes, G. Das, D. Gohl, M. Silies, S. Certel, S. Waddell, Layered reward signalling through octopamine and dopamine in *Drosophila*. *Nature* **492**, 433–437 (2012).

96. H. Youn, C. Kirkhart, J. Chia, K. Scott, A subset of octopaminergic neurons that promotes feeding initiation in *Drosophila melanogaster*. *PLOS ONE* **13**, e0198362 (2018).

97. S. Sayin, J.-F. De Backer, K. P. Siju, M. E. Wosniack, L. P. Lewis, L.-M. Frisch, B. Gansen, P. Schlegel, A. Edmondson-Stait, N. Sharifi, C. B. Fisher, S. A. Calle-Schuler, J. S. Lauritzen, D. D. Bock, M. Costa, G. S. X. E. Jefferis, J. Gjorgjieva, I. C. Grunwald Kadow, A neural circuit arbitrates between persistence and withdrawal in hungry *Drosophila*. *Neuron* **104**, 544–558.e6 (2019).

98. Y. Aso, D. Hattori, Y. Yu, R. M. Johnston, N. A. Iyer, T.-T. Ngo, H. Dionne, L. F. Abbott, R. Axel, H. Tanimoto, G. M. Rubin, The neuronal architecture of the mushroom body provides a logic for associative learning. *eLife* **3**, e04577 (2014).

99. F. Li, J. W. Lindsey, E. C. Marin, N. Otto, M. Dreher, G. Dempsey, I. Stark, A. S. Bates, M. W. Pleijzier, P. Schlegel, A. Nern, S. Takemura, N. Eckstein, T. Yang, A. Francis, A. Braun, R. Parekh, M. Costa, L. K. Scheffer, Y. Aso, G. S. Jefferis, L. F. Abbott, A. Litwin-Kumar, S. Waddell, G. M. Rubin, The connectome of the adult *Drosophila* mushroom body provides insights into function. *eLife* **9**, e62576 (2020).

100. A. Crocker, M. Shahidullah, I. B. Levitan, A. Sehgal, Identification of a neural circuit that underlies the effects of octopamine on sleep:wake behavior. *Neuron* **65**, 670–681 (2010).

101. E. E. LeDue, K. Mann, E. Koch, B. Chu, R. Dakin, M. D. Gordon, Starvation-induced depotentiation of bitter taste in *Drosophila*. *Curr. Biol.* **26**, 2854–2861 (2016).

102. P. Schlegel, A. S. Bates, T. Sturner, S. R. Jagannathan, N. Drummond, J. Hsu, L. Serratosa Capdevila, A. Javier, E. C. Marin, A. Barth-Maron, I. F. Tamimi, F. Li, G. M. Rubin, S. M. Plaza, M. Costa, G. S. X. E. Jefferis, Information flow, cell types and stereotypy in a full olfactory connectome. *eLife* **10**, e66018 (2021).

103. A. C. Groth, M. Fish, R. Nusse, M. P. Calos, Construction of transgenic *Drosophila* by using the site-specific integrase from phage phiC31. *Genetics* **166**, 1775–1782 (2004).

104. B. D. Pfeiffer, T.-T. Ngo, K. L. Hibbard, C. Murphy, A. Jenett, J. W. Truman, G. M. Rubin, Refinement of tools for targeted gene expression in *Drosophila*. *Genetics* **186**, 735–755 (2010).

105. S. J. Gratz, F. P. Ukken, C. D. Rubinstein, G. Thiede, L. K. Donohue, A. M. Cummings, K. M. O'Connor-Giles, Highly specific and efficient CRISPR/Cas9-catalyzed homology-directed repair in *Drosophila*. *Genetics* **196**, 961–971 (2014).

106. A. Thomas, P.-J. Lee, J. E. Dalton, K. J. Nomie, L. Stoica, M. Costa-Mattioli, P. Chang, S. Nuzhdin, M. N. Arbeitman, H. A. Dierick, A versatile method for cell-specific profiling of translated mRNAs in *Drosophila*. *PLOS ONE* **7**, e40276 (2012).

107. S.-J. Lee, H. Xu, C. Montell, Rhodopsin kinase activity modulates the amplitude of the visual response in *Drosophila*. *Proc. Natl. Acad. Sci. U.S.A.* **101**, 11874–11879 (2004).

108. T. Hummel, M. L. Vasconcelos, J. C. Clemens, Y. Fishilevich, L. B. Vosshall, S. L. Zipursky, Axonal targeting of olfactory receptor neurons in *Drosophila* is controlled by Dscam. *Neuron* **37**, 221–231 (2003).

109. A. Nern, B. D. Pfeiffer, G. M. Rubin, Optimized tools for multicolor stochastic labeling reveal diverse stereotyped cell arrangements in the fly visual system. *Proc. Natl. Acad. Sci. U.S.A.* **112**, E2967–2976 (2015).

110. K. Asahina, K. Watanabe, B. J. Duistermars, E. Hoopfer, C. R. Gonzalez, E. A. Eyjolfsdottir, P. Perona, D. J. Anderson, Tachykinin-expressing neurons control male-specific aggressive arousal in *Drosophila*. *Cell* **156**, 221–235 (2014).

111. H. K. Inagaki, Y. Jung, E. D. Hoopfer, A. M. Wong, N. Mishra, J. Y. Lin, R. Y. Tsien, D. J. Anderson, Optogenetic control of *Drosophila* using a red-shifted channelrhodopsin reveals experience-dependent influences on courtship. *Nat. Methods* **11**, 325–332 (2014).

112. K. Ishii, M. Wohl, A. DeSouza, K. Asahina, Sex-determining genes distinctly regulate courtship capability and target preference via sexually dimorphic neurons. *eLife* **9**, e52701 (2020).

113. K. Keleman, S. Kruttner, M. Alenius, B. J. Dickson, Function of the *Drosophila* CPEB protein Orb2 in long-term courtship memory. *Nat. Neurosci.* **10**, 1587–1593 (2007).

114. A. A. Robie, A. D. Straw, M. H. Dickinson, Object preference by walking fruit flies, *Drosophila melanogaster*, is mediated by vision and graviperception. *J. Exp. Biol.* **213**, 2494–2506 (2010).

115. S. Agrawal, M. H. Dickinson, The effects of target contrast on *Drosophila* courtship. *J. Exp. Biol.* **222**, jeb203414 (2019).

116. Y. Pan, G. W. Meissner, B. S. Baker, Joint control of *Drosophila* male courtship behavior by motion cues and activation of male-specific P1 neurons. *Proc. Natl. Acad. Sci. U.S.A.* **109**, 10065–10070 (2012).

117. S. R. Datta, D. J. Anderson, K. Branson, P. Perona, A. Leifer, Computational neuroethology: A call to action. *Neuron* **104**, 11–24 (2019).

118. H. Li, F. Horns, B. Wu, Q. Xie, J. Li, T. Li, D. J. Luginbuhl, S. R. Quake, L. Luo, Classifying *Drosophila* olfactory projection neuron subtypes by single-cell RNA sequencing. *Cell* **171**, 1206–1220.e22 (2017).

119. L. van der Maaten, G. Hinton, Visualizing data using t-SNE. *J. Mach. Learn. Res.* **9**, 2579–2605 (2008).

120. L. Luo, Y. J. Liao, L. Y. Jan, Y. N. Jan, Distinct morphogenetic functions of similar small GTPases: *Drosophila* Drac1 is involved in axonal outgrowth and myoblast fusion. *Genes Dev.* **8**, 1787–1802 (1994).

121. N. Yapici, Y.-J. Kim, C. Ribeiro, B. J. Dickson, A receptor that mediates the post-mating switch in *Drosophila* reproductive behaviour. *Nature* **451**, 33–37 (2008).

122. M. D. Gordon, K. Scott, Motor control in a *Drosophila* taste circuit. *Neuron* **61**, 373–384 (2009).

123. R. A. Baines, L. Seugnet, A. Thompson, P. M. Salvaterra, M. Bate, Regulation of synaptic connectivity: Levels of fasciclin II influence synaptic growth in the *Drosophila* CNS. *J. Neurosci.* **22**, 6587–6595 (2002).

124. C. R. von Reyn, P. Breads, M. Y. Peek, G. Z. Zheng, W. R. Williamson, A. L. Yee, A. Leonardo, G. M. Card, A spike-timing mechanism for action selection. *Nat. Neurosci.* **17**, 962–970 (2014).

125. B. D. Pfeiffer, J. W. Truman, G. M. Rubin, Using translational enhancers to increase transgene expression in *Drosophila*. *Proc. Natl. Acad. Sci. U.S.A.* **109**, 6626–6631 (2012).

126. R. A. Bohm, W. P. Welch, L. K. Goodnight, L. W. Cox, L. G. Henry, T. C. Gunter, H. Bao, B. Zhang, A genetic mosaic approach for neural circuit mapping in *Drosophila*. *Proc. Natl. Acad. Sci. U.S.A.* **107**, 16378–16383 (2010).

127. N. C. Klapoetke, Y. Murata, S. S. Kim, S. R. Pulver, A. Birdsey-Benson, Y. K. Cho, T. K. Morimoto, A. S. Chuong, E. J. Carpenter, Z. Tian, J. Wang, Y. Xie, Z. Yan, Y. Zhang, B. Y. Chow, B. Surek, M. Melkonian, V. Jayaraman, M. Constantine-Paton, G. K.-S. Wong, E. S. Boyden, Independent optical excitation of distinct neural populations. *Nat. Methods* **11**, 338–346 (2014).

128. P. Stockinger, D. Kvitsiani, S. Rotkopf, L. Tirián, B. J. Dickson, Neural circuitry that governs *Drosophila* male courtship behavior. *Cell* **121**, 795–807 (2005).

129. E. J. Rideout, A. J. Dornan, M. C. Neville, S. Eadie, S. F. Goodwin, Control of sexual differentiation and behavior by the *doublesex* gene in *Drosophila melanogaster*. *Nat. Neurosci.* **13**, 458–466 (2010).

130. J. Y. Yu, M. I. Kanai, E. Demir, G. S. X. E. Jefferis, B. J. Dickson, Cellular organization of the neural circuit that drives *Drosophila* courtship behavior. *Curr. Biol.* **20**, 1602–1614 (2010).

131. H. Toda, X. Zhao, B. J. Dickson, The *Drosophila* female aphrodisiac pheromone activates *ppk23*(+) sensory neurons to elicit male courtship behavior. *Cell Rep.* **1**, 599–607 (2012).

132. E. Starostina, T. Liu, V. Vijayan, Z. Zheng, K. K. Siwicki, C. W. Pikielny, A *Drosophila* DEG/EnaC subunit functions specifically in gustatory neurons required for male courtship behavior. *J. Neurosci.* **32**, 4665–4674 (2012).

133. J. Schindelin, I. Arganda-Carreras, E. Frise, V. Kaynig, M. Longair, T. Pietzsch, S. Preibisch, C. Rueden, S. Saalfeld, B. Schmid, J.-Y. Tinevez, D. J. White, V. Hartenstein, K. Eliceiri, P. Tomancak, A. Cardona, Fiji: An open-source platform for biological-image analysis. *Nat. Methods* **9**, 676–682 (2012).

134. Y. Wan, H. Otsuna, H. A. Holman, B. Bagley, M. Ito, A. K. Lewis, M. Colasanto, G. Kardon, K. Ito, C. Hansen, FluoRender: Joint freehand segmentation and visualization for many-channel fluorescence data analysis. *BMC Bioinformatics* **18**, 280 (2017).

135. M. Kabra, A. A. Robie, M. Rivera-Alba, S. Branson, K. Branson, JAABA: Interactive machine learning for automatic annotation of animal behavior. *Nat. Methods* **10**, 64–67 (2013).

136. A. Dobin, C. A. Davis, F. Schlesinger, J. Drenkow, C. Zaleski, S. Jha, P. Batut, M. Chaisson, T. R. Gingeras, STAR: Ultrafast universal RNA-seq aligner. *Bioinformatics* **29**, 15–21 (2013).

137. S. Heinz, C. Benner, N. Spann, E. Bertolino, Y. C. Lin, P. Laslo, J. X. Cheng, C. Murre, H. Singh, C. K. Glass, Simple combinations of lineage-determining transcription factors prime cis-regulatory elements required for macrophage and B cell identities. *Mol. Cell* **38**, 576–589 (2010).

138. M. D. Robinson, D. J. McCarthy, G. K. Smyth, edgeR: A Bioconductor package for differential expression analysis of digital gene expression data. *Bioinformatics* **26**, 139–140 (2010).